

Thermodynamics of Interacting Fermions in Atomic Traps

Qijin Chen, Jelena Stajic,* and K. Levin

James Franck Institute and Department of Physics, University of Chicago, Chicago, Illinois 60637

(Dated: March 21, 2018)

We calculate the entropy in a trapped, resonantly interacting Fermi gas as a function of temperature for a wide range of magnetic fields between the BCS and Bose-Einstein condensation endpoints. This provides a basis for the important technique of adiabatic sweep thermometry, and serves to characterize quantitatively the evolution and nature of the excitations of the gas. The results are then used to calibrate the temperature in several ground breaking experiments on ${}^6\text{Li}$ and ${}^{40}\text{K}$.

PACS numbers: 03.75.Hh, 03.75.Ss, 74.20.-z

Phys. Rev. Lett. **95**, 260405 (2005)

The claims [1, 2, 3, 4, 5] that superfluidity has been observed in fermionic atomic gases have generated great excitement. Varying a magnetic field, one effects a smooth evolution from BCS superfluidity to Bose-Einstein condensation (BEC) [6, 7]. In this Letter we use a BCS-BEC crossover theory to study the entropy S over the entire experimentally accessible crossover regime. Our goal is to help establish a methodology for obtaining the temperature T of a strongly interacting Fermi gas via adiabatic sweeps. This addresses an essential need of the experimental cold atom community by providing a temperature calibration for their ground breaking experiments [2, 8, 9]. In the process, we characterize quantitatively the evolution of the excitations and show how their character evolves smoothly from fermionic to bosonic, and conversely.

In adiabatic sweeps, the starting T at either a BEC or BCS endpoint is estimated from the “known” shape of the profile in the trapped cloud. Then, the temperature (near unitarity, say) is obtained by equating the entropy before the sweep to that in the strongly interacting regime after the sweep. Conventionally, the temperature scale which appears in the superfluid phase diagram [2, 8] involves an isentropic sweep between the unitary and the non-interacting Fermi gas regimes. The direction of the sweep is irrelevant in these reversible processes. The important experimental phase diagrams plot the condensate fraction, N_s/N near unitarity vs this Fermi gas-projected temperature, T_{eff} .

In this paper, our thermodynamical calculations are used to relate the actual physical temperatures T to T_{eff} , where, in general, T is significantly greater than T_{eff} . A calculation of $N_s(T)$ is simultaneously undertaken [10, 11] which provides an important self-consistency condition on the thermodynamics, since the same excitations appear in both. Moreover, a calculation of N_s has to be done with proper attention paid to collective modes and gauge invariance [12]. Here we address the various condensate fractions found experimentally [1, 2], (with emphasis on ${}^6\text{Li}$), as a function of T_{eff} , in the experimental range of magnetic fields.

Our work is based on the BCS-Leggett ground state [6, 7] and its finite T extension [11]. Four different classes of experiments have been successfully addressed in this framework. These include (i) $T \approx 0$ breathing modes experiments [3, 4] and theory [13, 14], (ii) radio frequency (RF) pairing gap ex-

periments [9] and theory [15, 16], and (iii) T -dependent density profiles [17]. Finally, (iv) plots of the energy E vs T at unitarity [18] yield very good agreement with experiment and serve to calibrate the present thermometry. Two well-known weaknesses of the mean field approach (an underestimate of β and an overestimate of the inter-boson scattering length a_B in the deep BEC regime) should be noted. The first affects $E(T)$ but not $S(T)$. However, for the second we introduce a caveat: if the initial endpoint of sweep thermometry is sufficiently deep in the BEC regime (say, $k_F a \leq 0.3$) the accuracy of the final temperature, we calculate for the unitary regime, could be improved by computing the initial S in the deep BEC regime using a pure-boson model with a_B set by hand to the Petrov result [19].

Because previous thermodynamic theories did not address unitarity, it has not been possible until now to arrive at a temperature scale in the experimentally interesting resonant superfluid regime. Carr *et al.* [20, 21] calculated S at the BCS and weakly interacting, deep-BEC endpoints. The latter true Bose limit which they considered does not appear to be appropriate to current collective mode experiments, [3, 4], which show [13, 14] that for physically accessible (i.e., near-BEC) fields, fermions are playing an important role. Thus, the BCS-Leggett ground state appears to be more appropriate than one deriving from Bose-liquid-based theory. Williams *et al.* [22] calculated S for a BCS-BEC crossover theory using a mixture of noninteracting fermions and bosons [22]. This work, omits the important and self consistently determined fermionic excitation gap Δ which is an essential component for describing the thermodynamics of fermionic superfluids.

Our thermodynamical calculations focus on this self-consistently determined Δ ; they are based, for completeness, on a two-channel Hamiltonian [11, 23, 24]. Here Δ appears in the fermionic dispersion $E_{\mathbf{k}} = \sqrt{(\epsilon_{\mathbf{k}} - \mu)^2 + \Delta^2}$. (We define $\epsilon_{\mathbf{k}} = \hbar^2 k^2 / 2m$ as the kinetic energy of free atoms, and μ the fermionic chemical potential.) Importantly, this Δ provides a measure of bosonic degrees of freedom. In the fermionic regime ($\mu > 0$), Δ is just the energy required to dissociate the pairs and thereby excite fermions. At finite T , the closed-channel molecular bosons and the open-channel finite momentum Cooper pairs are strongly hybridized with each other, making up the “bosonic” excitations which contribute to thermodynamics.

Our many-body formalism has been described below the superfluid transition temperature T_c [11]. The parameter Δ , (when squared), is the analogue of the total number of particles, in the simplest theory of BEC. Just as in BEC, there are two self-consistency conditions: (i) the effective chemical potential of the pairs, μ_{pair} , is zero, for $T \leq T_c$ (as is that of the closed-channel molecular bosons μ_{mb}), and, (ii) the number of pairs, reflected in $\Delta^2(T)$ contains two additive contributions representing condensed ($\tilde{\Delta}_{sc}^2$) and noncondensed (Δ_{pg}^2) pairs. The first condition implies that $\Delta(T)$ satisfies a BCS-like gap equation. Then, the condensate is deduced, just as in BEC, by determining the difference between Δ^2 and Δ_{pg}^2 . In this approach the hybridized pairs have dispersion $\Omega_{\mathbf{q}} = \hbar^2 q^2 / 2M^*$, with effective pair mass M^* .

We now extend this approach above T_c . Our first equation represents the important defining condition on μ_{pair} : that the inverse pair propagator (or T -matrix) $t^{-1}(Q)|_{Q=0} = Z\mu_{pair}$, with (inverse) “residue” Z . While in the superfluid regions μ_{pair} and μ_{mb} vanish, in general, we have

$$U_{eff}^{-1}(0) + \sum_{\mathbf{k}} \frac{1 - 2f(E_{\mathbf{k}})}{2E_{\mathbf{k}}} = Z\mu_{pair}, \quad (1)$$

where $U_{eff}(0) = U + g^2/(2\mu - \nu)$ involves the sum of the direct attraction U between open-channel fermions, as well as the virtual processes associated with the Feshbach resonance. Here $f(x)$ is the Fermi distribution function. The determination of the inter-channel coupling constant, g , and the magnetic field detuning, ν , is described elsewhere [25], as are the residues Z and Z_b [11]. The contribution from hybridized bosons will lead to a normal state excitation gap [9, 11, 26, 27] or pseudogap (pg). This can be written in terms of the Bose distribution function $b(x)$ as

$$\Delta_{pg}^2 = Z^{-1} \sum_{\mathbf{q}} b(\Omega_{\mathbf{q}} - \mu_{pair}). \quad (2)$$

We use the local density approximation (LDA) throughout with a harmonic trap potential $V(r)$. For notational simplicity, we omit writing $V(r)$ in favor of $\mu(r)$ according to the LDA prescription: $\mu \rightarrow \mu(r) \equiv \mu - V(r)$, where $\mu \equiv \mu(0)$. The total atomic number $N \equiv \int d^3r n(r)$, where

$$n = 2n_{b0} + 2Z_b^{-1} \sum_{\mathbf{q}} b(\Omega_{\mathbf{q}} - \mu_{mb}) + 2 \sum_{\mathbf{k}} [v_{\mathbf{k}}^2(1 - f(E_{\mathbf{k}})) + u_{\mathbf{k}}^2 f(E_{\mathbf{k}})]. \quad (3)$$

Here $n_{b0} = g^2 \Delta_{sc}^2 / [(\nu - 2\mu(r))U]^2$ is the density of condensed closed-channel molecules, and $u_{\mathbf{k}}^2, v_{\mathbf{k}}^2 = [1 \pm (\epsilon_{\mathbf{k}} - \mu(r))/E_{\mathbf{k}}]/2$. The total order parameter [23, 24, 26] is given by $\tilde{\Delta}_{sc} = \Delta_{sc} + |g|\sqrt{n_{b0}}$.

To make progress, we numerically solve Eqs. (1)-(2) at each r for given μ and then self-consistently adjust μ via the total number constraint. Next we obtain the entropy S directly from the thermodynamical potential [28]. This potential contains fermionic contributions from bare fermions, Ω_f , and bosonic

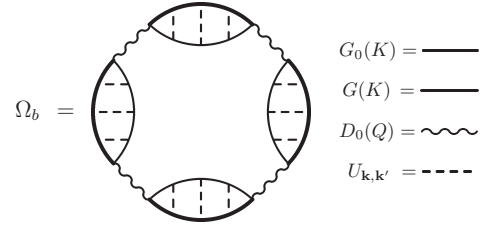


FIG. 1: Bosonic contribution to the thermodynamical potential. Here G_0 (G) and D_0 (D) are the “bare” (“full”) propagators associated with the fermions and closed-channel molecular bosons, respectively, K and Q are four-momenta, and $U_{\mathbf{k},\mathbf{k}'}$ is the open-channel pairing interaction.

contributions Ω_b . The latter is given by the sum of all possible ring diagrams shown in Fig. 1. It can be easily shown that this Ω_b is consistent with the self energy diagrams for the fermions and the molecular bosons. After regrouping, we see that S has two contributions, from fully dressed fermions (S_f) and from their bosonic counterpart (S_b). The total entropy involves an integral over the trap, given by $S = \int d^3r s(r)$ (and similarly for S_f and S_b), where

$$\begin{aligned} s &= s_f + s_b, \\ s_f &= -2 \sum_{\mathbf{k}} [f_{\mathbf{k}} \ln f_{\mathbf{k}} + (1 - f_{\mathbf{k}}) \ln(1 - f_{\mathbf{k}})], \\ s_b &= - \sum_{q \neq 0} [b_q \ln b_q - (1 + b_q) \ln(1 + b_q)], \end{aligned} \quad (4)$$

where $f_{\mathbf{k}} \equiv f(E_{\mathbf{k}})$, and $b_q \equiv b(\Omega_{\mathbf{q}} - \mu_{mb})$; a relatively small contribution associated with the T dependence of $\Omega_{\mathbf{q}}$ has been dropped. The fermion contribution coincides formally with the standard BCS result for noninteracting quasiparticles [although here $\Delta(T_c) \neq 0$]. And the bosonic contribution is given by the expression for non-directly-interacting bosons with dispersion $\Omega_{\mathbf{q}}$. These bosons are not free, however; because of interactions with the fermions, their propagator contains important self-energy and mass renormalization effects.

Figure 2 illustrates the behavior of S as a function of T obtained from our self-consistent equations, over the entire experimentally relevant crossover regime. The magnetic field is contained in the parameter $1/k_F a$, which increases with decreasing field. Here a is the s -wave fermionic scattering length, k_F is the Fermi wavevector at the trap center, and $k_B T_F = \hbar^2 k_F^2 / 2m$ is the noninteracting Fermi temperature. Two important aspects of the fermionic contribution S_f should be noted. Generally, the fermions have a gap Δ in their excitation spectrum (which increases with decreasing field) and moreover this T dependent gap is inhomogeneous so that the fermions near the trap edge often behave as free particles at $T > \Delta$. These quasi-“free” fermions change the T dependence of S_f from exponential to power law. They have also been seen in RF experiments [9, 15], as a free fermion peak in the spectra.

We refer to Fig. 2, starting from the high field or BCS regime where S is linear in T . As the field is lowered to-

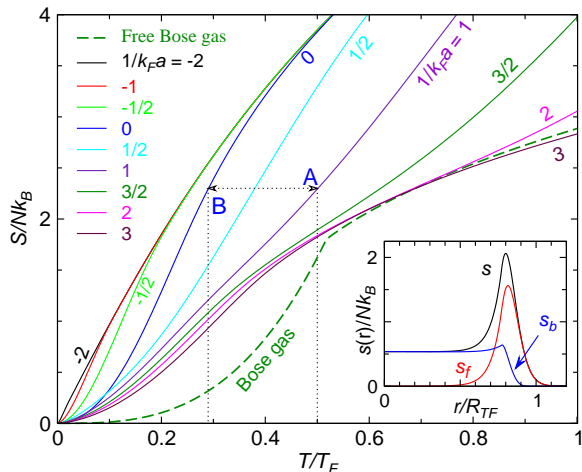


FIG. 2: (color online) Entropy per atom as a function of T for different values of $1/k_F a$ from BCS to BEC in a harmonic trap. The dotted lines show an isentropic sweep between $1/k_F a = 1$ and unitarity. For comparison, we also plot S for an ideal Bose gas (dashed line). The $1/k_F a = 3$ curve lies below the dashed line at $T > 0.8T_F$ reflects that $M^* \neq 2m$. The inset plots the spatial profile of total entropy s (black curve) and its fermionic (s_f , red) and bosonic (s_b , blue) component contributions at unitarity for $T = T_c/4$. Here R_{TF} is the Thomas-Fermi radius, and $T_c = 0.27T_F$.

wards unitarity, S_f will vary as a low- T power law which is higher than linear. Simultaneously, the bosonic degrees of freedom emerge. Here one sees a $T^{3/2}$ power law from these excited bosons. At unitarity, bosonic effects dominate for $T/T_F \lesssim 0.05$ or $T/T_c \lesssim 0.2$. For an extended range of $T < T_c$, the fermions and bosons combine to yield, $S \propto T^2$, which can be compared with the experimental power law [18] $T^{2.73}$. Finally in the near-BEC regime one sees an essentially pure bosonic $T^{3/2}$ power law in S at low T in the superfluid phase. The relative contribution of the bosonic excitations, S_b/S evolves continuously from 0 to 1 as $1/k_F a$ increases from $-\infty$ to $+\infty$. S becomes dominantly bosonic once μ becomes negative.

The bosonic $T^{3/2}$ power law found in the trap is the same as found for the homogeneous situation. Inhomogeneity effectively disappears here because the fermion-boson interactions lead to the self-consistent constraint that $\mu_{pair} = 0$ for the entire superfluid region. This same disappearance of inhomogeneity is found in Ref. [20]. This is different from a strictly non-interacting Bose system [22] (dashed line in Fig. 2) where one does not have a vanishing boson chemical potential below T_c except at the trap center. The previous work of Ref. [20] is based on interacting but true bosons. The present situation is more complex since Cooper pair operators do not obey Bose commutation relations, (nor does the linear combination of Cooper pair and closed-channel boson operators). This suggests that a theory based on a true Bose liquid may not be appropriate for the fields that have been accessed experimentally. Moreover, if one were to contemplate contributions from the linearly dispersing Goldstone bosons, albeit within a more

general ground state, their contribution, at unitarity, will not be as important as that from the edge fermions.

To shed additional light on the component fermionic and bosonic contributions, in the inset to Fig. 2 we decompose the various terms in the entropy to reveal their spatial distributions, for the unitary case at $T = T_c/4$. It can be seen that the fermionic contribution s_f (red curve) is limited to the trap edge, where Δ is small. By contrast, the bosonic contribution s_b (blue curve) is evenly distributed over the superfluid region and rapidly decays at larger radii.

Figure 2 provides a basis for thermometry in adiabatic sweep experiments. The vertical lines illustrate how to choose an initial temperature ($T_i = 0.5T_F$ at point “A”) with an initial value of $1/k_F a (=1)$ and use an isentropic sweep (represented by the horizontal line through “A” and “B”) to obtain the final temperature ($T_f = 0.28T_F$ at point “B”) with the final value of $1/k_F a (=0)$. It is most convenient to begin with either the BCS regime or BEC regimes, since here T_i can, in principle, be determined by fitting the density profiles.

Figure 3 presents a plot of the superfluid fraction [10, 11] N_s/N in the intermediate regime as a function of an effective temperature T_{eff}/T_F for different values of initial fields or $1/k_F a$. Here T_{eff} is the temperature reached after an adiabatic sweep to a BCS-like state. Based on experiment, we take the final state as $1/k_F a = -0.59$ at 1025 G for ${}^6\text{Li}$ [2] and a noninteracting Fermi gas for ${}^{40}\text{K}$ [8].

The same vertical axis appears in the inset but with the physical temperature scale T , so that this figure provides a means of directly calibrating the temperature scale T_{eff} which has been used in the important phase diagrams of ${}^6\text{Li}$ and ${}^{40}\text{K}$. Figure 3 also provides a means of comparing the condensate fractions with those in the phase diagrams. For ${}^6\text{Li}$ at 900 G, with $T_{\text{eff}}/T_F = 0.2, 0.1$ and 0.05 , the experimental condensate fractions are 0.0, 0.1 and 0.6. This should be compared with our calculated values, 0.006 0.36, and 0.73, respectively. For ${}^6\text{Li}$ at 770 G, the condensate first appears at $T_{\text{eff}}/T_F = 0.18$, consistent with theory. From the values of $k_F a$ and T_c at both ends (importantly, the latter can be read from the inset), one can easily see that the sweep from 770 G to 1025 G is still very far from a full BEC-BCS sweep.

There are two reasons for the larger condensate fractions found theoretically for ${}^6\text{Li}$. A calculation of the BEC-like density profiles shows that the noncondensed pairs inside the superfluid region have a flat density distribution, which reflects the vanishing of μ_{pair} [17]. The superfluid fraction extracted experimentally (assuming a Gaussian form for the noncondensed particles inside the condensate core) is, thus, underestimated, most notably around $T_c/2$. In addition, earlier work [18] shows that when the system is treated as a non-interacting Fermi gas, T_{eff} will be underestimated whenever a condensate is present (at $T < T_c \approx 0.17T_F$ at 1025 G). This suggests that theory and experiment can be brought into rather good agreement for the case of ${}^6\text{Li}$. For ${}^{40}\text{K}$, one has to appeal to non-adiabaticity and other complications of the sweep process to understand the small measured fractions.

For this case, we emphasize temperature scales. For a full

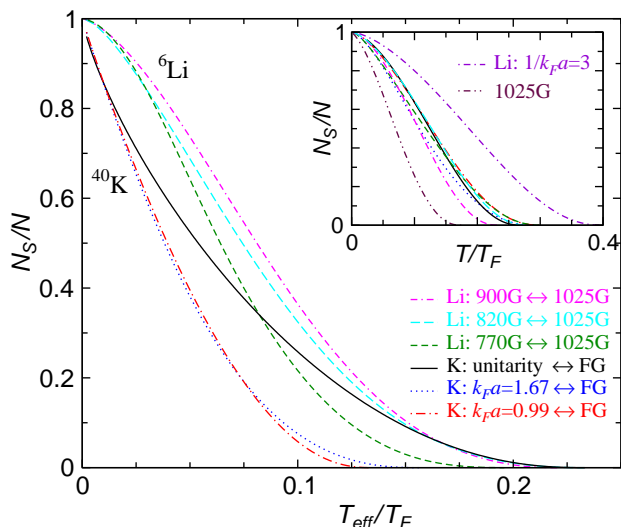


FIG. 3: (color online) Superfluid density N_s/N at different magnetic fields for ${}^6\text{Li}$ and ${}^{40}\text{K}$ as a function of the effective temperature, T_{eff} , measured in a near-BCS (at 1025G for ${}^6\text{Li}$) or noninteracting Fermi gas (FG, ${}^{40}\text{K}$) state accessed via reversible adiabatic sweeps of magnetic field. The inset plots the same N_s/N as a function of the physical temperature at each field value. The system is not far from the resonance in these states. Also plotted in the inset is $N_s(T)/N$ at 1025G and $1/k_F a = 3$ for ${}^6\text{Li}$. The values of field and $k_F a$ were chosen based on Refs. [2] and [8]. For ${}^6\text{Li}$, $T_F = 3.6\mu\text{K}$, so that $1/k_F a = -0.59, -0.26, 0.07, 0.38$ for 1025 G, 900 G, 820 G and 770 G, respectively.

BCS to near-BEC [$(k_F a)_{\text{final}} = 1.7$] adiabatic sweep [8] with initial $T_{\text{eff}} \equiv T_i = 0.19T_F$, the final reported temperatures in experiment [8] and in theory are $T_f = 0.47T_F$ and $0.33T_F$, respectively. For the same $(k_F a)_{\text{final}}$ but with $T_i = 0.17T_F$, we find $T_f \approx T_c$, in agreement with the observed sudden onset of a bimodal distribution in the density profile. Similarly for a sweep from a Fermi gas down to $(k_F a)_{\text{final}} = 0.99$ with $T_i = 0.06T_F$, the experimentally quoted and theoretically calculated T_f are $0.25T_F$ and $0.18T_F$, respectively. The experimental sweeps were not strictly adiabatic [8], so that the experimental T_f should serve as upper bounds. Our calculations are more consistent with experiment, than if one had presumed a T^3 power law for S in the BEC regime, from which one would infer $T_f = 0.52T_F$ and $0.37T_F$, respectively, exceeding the upper bounds.

Experimentally, ${}^{40}\text{K}$ gases [8] are prepared in the noninteracting limit, where, as a result of heating associated with an adiabatic sweep, low T is difficult to reach. By contrast ${}^6\text{Li}$ gases [2, 4] are prepared in the BEC regime, so that higher condensate fractions of 80% and 95% have been reported [2, 4, 9] near unitarity via adiabatic cooling. Finally, we note that the rather large $T_c \approx 0.17T_F$ at 1025 G makes it hard to access the Fermi gas regime in ${}^6\text{Li}$. This may be circumvented either by reduction in the size of N or T_F or, possibly, by sweeps to 528 G [29]. In ${}^{40}\text{K}$, one avoids this problem altogether.

Without knowing the temperature, measurements in this

field cannot be directly compared to any theory. The present work presents a theory for the entropy S of a Fermi gas, at general accessible magnetic fields, which thereby calibrates T in various existing [2, 8, 9] and future experiments.

We are extremely grateful to J.E. Thomas, J. Kinast and A. Turlapov for many helpful discussions, and to N. Nygaard, C. Chin, M. Greiner, C. Regal, D.S. Jin, and M. Zwierlein as well. This work was supported by NSF-MRSEC Grant No. DMR-0213745 and by the Institute for Theoretical Sciences and DOE, No. W-31-109-ENG-38 (QC).

* Present address: Los Alamos Nat'l Lab, Los Alamos, NM 87545

- [1] C. A. Regal, M. Greiner, and D. S. Jin, Phys. Rev. Lett. **92**, 040403 (2004).
- [2] M. W. Zwierlein et al., Phys. Rev. Lett. **92**, 120403 (2004).
- [3] J. Kinast et al., Phys. Rev. Lett. **92**, 150402 (2004).
- [4] M. Bartenstein et al., Phys. Rev. Lett. **92**, 203201 (2004).
- [5] M. W. Zwierlein, J. R. Abo-Shaeer, A. Schirotzek, and W. Ketterle, Nature **435**, 1047 (2005).
- [6] D. M. Eagles, Phys. Rev. **186**, 456 (1969).
- [7] A. J. Leggett, in *Modern Trends in the Theory of Condensed Matter* (Springer-Verlag, Berlin, 1980), pp. 13–27.
- [8] M. Greiner, C. A. Regal, and D. S. Jin, Nature **426**, 537 (2003).
- [9] C. Chin et al., Science **305**, 1128 (2004).
- [10] Defining the condensate fraction in the fermionic regime is not unambiguous. N_s/N which we use here gives the largest possible fraction.
- [11] Q. J. Chen, J. Stajic, S. N. Tan, and K. Levin, Phys. Rep. **412**, 1 (2005).
- [12] I. Kosztin, Q. J. Chen, Y.-J. Kao, and K. Levin, Phys. Rev. B **61**, 11662 (2000).
- [13] H. Hu et al., Phys. Rev. Lett. **93**, 190403 (2004).
- [14] H. Heiselberg, Phys. Rev. Lett. **93**, 040402 (2004).
- [15] J. Kinnunen, M. Rodriguez, and P. Törmä, Science **305**, 1131 (2004).
- [16] Y. He, Q. J. Chen, and K. Levin, Phys. Rev. A **72**, 011602(R) (2005).
- [17] J. Stajic, Q. J. Chen, and K. Levin, Phys. Rev. Lett. **94**, 060401 (2005).
- [18] J. Kinast, A. Turlapov, J. E. Thomas, Q. J. Chen, J. Stajic, and K. Levin, Science **307**, 1296 (2005).
- [19] D. S. Petrov, C. Salomon, and G. V. Shlyapnikov, Phys. Rev. Lett. **93**, 090404 (2004).
- [20] L. D. Carr, G. V. Shlyapnikov, and Y. Castin, Phys. Rev. Lett. **92**, 150404 (2004).
- [21] L. D. Carr, R. Chiamonte, and M. J. Holland, Phys. Rev. A **70**, 043609 (2004).
- [22] J. E. Williams, N. Nygaard, and C. W. Clark, New J. Phys. **6**, 123 (2004).
- [23] Y. Ohashi and A. Griffin, Phys. Rev. Lett. **89**, 130402 (2002).
- [24] J. N. Milstein, S. J. J. M. F. Kokkelmans, and M. J. Holland, Phys. Rev. A **66**, 043604 (2002).
- [25] Q. J. Chen and K. Levin, Phys. Rev. Lett. **95**, 260406 (2005).
- [26] J. Stajic et al., Phys. Rev. A **69**, 063610 (2004).
- [27] M. Greiner, C. A. Regal, and D. S. Jin, Phys. Rev. Lett. **94**, 070403 (2005).
- [28] Q. J. Chen, K. Levin, and I. Kosztin, Phys. Rev. B **63**, 184519 (2001).
- [29] K. M. O'Hara et al., Science **298**, 2179 (2002).